Ecological Informatics 91 (2025) 103436

Contents lists available at ScienceDirect

Ecological Informatics

journal homepage: www.elsevier.com/locate/ecolinf

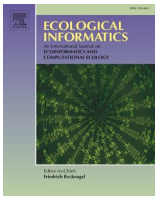

Shoreline dynamics of barrier islands in the Gulf of Mexico: A 30-year comparative analysis of developed vs. undeveloped islands

SaMin Han *, Timothy J. Schauwecker

Department of Landscape Architecture and Environmental Design, College of Agriculture and Life Sciences, Mississippi Agricultural and Forestry Experiment Station, Mississippi State University, MS State, MS, USA

ARTICLE INFO

Keywords:
Barrier islands
Shoreline change
Development impacts
Gulf of Mexico
Digital shoreline analysis system

ABSTRACT

Barrier islands protect mainland coasts by absorbing wave and tidal energy, reducing storm impacts, and preserving coastal ecosystems. The barrier islands along the Alabama and Mississippi coast of the Gulf of Mexico, including Dauphin, Petit Bois, and Horn Islands, face frequent hurricanes and climate pressures. Among them, Dauphin Island is developed, while Petit Bois and Horn Islands remain relatively undisturbed, allowing for a comparative study of human development impacts on shoreline dynamics.

Using the Digital Shoreline Analysis System, we evaluated 618 transects derived from aerial, satellite, and LiDAR data spanning 1984–2015. Three shoreline-change indicators, Net Shoreline Movement, Shoreline Change Envelope, and Linear Regression Rate, were applied to both bay and coast sides of each island. Statistical comparisons (ANOVA and Tukey HSD) tested differences among islands. Results show Dauphin Island experienced chronic coast-side erosion and substantial bay-side deposition, indicating inland sediment migration. In contrast, Petit Bois showed net erosion on both sides, while Horn Island displayed balanced coast-side dynamics and lower rates of change. ANOVA confirmed significant inter-island differences ($p < 0.01$).

These findings demonstrate that intensive development accelerates shoreline retreat and disrupts sediment balance, whereas undeveloped islands retain greater geomorphic resilience. This study provides new empirical evidence of the long-term geomorphic consequences of human disturbance on Gulf Coast barrier islands and underscores the need for nature-based management strategies such as dune restoration and controlled development. Insights from this study will contribute to future coastal management, habitat restoration, and conservation strategies, offering guidance for policymakers to mitigate the negative effects of development on barrier island ecosystems.

1. Introduction

Barrier islands are dynamic landforms sculpted by waves, tides, and sediment processes. They play a vital role as natural buffers, protecting mainland coastlines from oceanic forces such as storm surges and tidal fluctuations (Han and Hogue, 2024; Miller et al., 2018; Sancho et al., 2011; Stallins, 2005). Rather than remaining static, barrier islands continuously evolve in response to environmental factors, including sea-level rise, hurricanes, storms, and storm events (Fernández-Montblanc et al., 2020). Their preservation is not only essential for mitigating coastal hazards and protecting the mainland, but also for sustaining offshore biodiversity and the ecosystem, such as through sediment trapping, organic accumulations, and shoreline stabilization (Bilskie et al., 2016; Durán and Moore, 2013; Fernández-Montblanc et al., 2020; Masselink et al., 2016; Smith et al., 2018).

This study conceptualizes barrier islands as coupled human–natural systems whose geomorphic trajectories are shaped by both environmental forces and anthropogenic disturbances (Hanley et al., 2014; Stallins, 2005). The barrier island chains along the Alabama and Mississippi coasts of the Gulf of Mexico have historically functioned as dynamic coastal buffers, absorbing wave energy and mitigating the impacts of tropical storms and tidal floods (Bilskie et al., 2016; Irish et al., 2010; Passeri et al., 2015). However, these systems are increasingly vulnerable to compounded stressors such as rising sea levels, intensified storm frequency, sediment supply reduction, and land-use changes. Morton (2008) documented the widespread morphological disintegration of Gulf Coast barrier islands, attributing it to long-term sediment deficits and the acceleration of sea-level rise. Byrnes et al.

* Corresponding author at: Box 9725, MS State, MS 39762-9725, USA.
E-mail address: sh2851@msstate.edu (S. Han).

https://doi.org/10.1016/j.ecoinf.2025.103436
Received 9 January 2025; Received in revised form 15 September 2025; Accepted 16 September 2025
Available online 17 September 2025

(2010) further highlighted the impact of 29 tropical storm events on Dauphin Island between 1944 and 2009, emphasizing the frequency of overwash and breaching, particularly on the island's western end.

Vegetation plays a critical role in mediating these geomorphic changes. Smith et al. (2018) demonstrated that vegetated dunes significantly enhance sediment stability and shoreline resilience, reinforcing the ecological importance of maintaining plant structure along dynamic coastal systems. Recent studies have also shown that vegetation dynamics are increasingly shaped by anthropogenic influence, including the spread of invasive species. For instance, Gornish and Miller (2022) and Schmid et al. (2024) revealed that non-native plants such as *Carex kobomugi* and *Hydrocotyle bonariensis* alter sediment accumulation and mobility by modifying below-ground biomass and organic matter content. These changes can disrupt the natural feedback mechanisms operating between vegetation and dune formation, leading to reduced geomorphic stability. Likewise, Seabloom et al. (2024) emphasized that invasive species reduce the functional diversity and resilience of native dune communities, ultimately diminishing their ability to trap sediment and resist storm-driven erosion. In the context of Dauphin Island, Han and Hogue (2024) found that increased development intensity has coincided with measurable declines in both vegetative maturity and dune cover, in contrast to the relatively undisturbed and structurally stable conditions on Horn and Petit Bois Islands. To systematically quantify long-term shoreline change, the Digital Shoreline Analysis System (DSAS) has emerged as a widely used geospatial tool for coastal researchers. Developed by the US Geological Survey (USGS), DSAS is an ArcGIS extension that calculates shoreline movement statistics by generating transects from a user-defined baseline across time-stamped shoreline positions (U.S. Geological Survey, 2023; Himmelstoss et al., 2018). DSAS has been applied effectively to a range of coastal environments to assess erosion and deposition patterns, evaluate the geomorphic effects of extreme events, and inform coastal management policies.

For example, Smith et al. (2018) used DSAS to evaluate shoreline trends on Dauphin Island over a 75-year period, capturing both high-energy storm impacts and long-term sediment shifts. Similarly, Henderson et al. (2017) demonstrated the value of combining DSAS with LiDAR and aerial imagery to map erosion hotspots and geomorphic recovery along the northern Gulf Coast. The tool's capacity to accommodate diverse spatial and temporal datasets has made it particularly valuable in studies seeking to understand the cumulative effects of human disturbance, storm frequency, and vegetation loss on shoreline stability. In the present study, DSAS was applied to compare developed and undeveloped barrier islands using consistent methods and uncertainty frameworks, offering a replicable approach to evaluating the intersection of anthropogenic activity and sedimentary dynamics.

Recent studies from other parts of India further illustrate the urgency of examining barrier island dynamics. Along Sagar Island in West Bengal, rapid shoreline retreat has led to the loss of nearly 30 km^2 of land over recent decades, while islands in Kerala such as Vypin, Vallarpadam, and Bolgatty have experienced predominantly accretional trends linked to port development and industrial activities (Chettiyam Thodi et al., 2023; Gopinath et al., 2023). These contrasting cases highlight the need for comparative analyses that distinguish the geomorphic responses of developed and undeveloped islands under varying natural and anthropogenic pressures.

Although precedent studies have established the influence of storms and sea-level rise on Dauphin Island, few have directly examined how human development correlates with spatial patterns of shoreline erosion and deposition, particularly distinguishing between the coast and bay sides. This study focuses on three barrier islands located on the Alabama-Mississippi border: Dauphin, Petit Bois, and Horn Islands (see Fig. 1). These islands share similar geographical features, geologies, and climates, and are exposed to similar climatic events in terms of

Fig. 1. Study area – Alabama-Mississippi barrier island chain: Dauphin, Petit Bois, and Horn Islands. The research area is located in the barrier island chain along the Gulf of Mexico, between the borders of Alabama and Mississippi. This study specifies two sides of the barrier islands: bay-side towards the mainland and coast-side towards the ocean (source: ArcGIS; coordinate system: WGS 1984 Web Mercator).

frequency and intensity. Of the three, only Dauphin Island is accessible by road and developed with vacation homes and retail establishments. In contrast, Petit Bois and Horn Islands are accessible only by boat, with no human-made structures. These two islands retain natural dune systems and unique ecology and serve as habitats for wildlife and migratory birds, as well as occasional recreational activities such as fishing. Such characteristics collectively establish the significance of both natural and anthropogenic drivers in shaping an island's morphology over time.

Thus, the primary objective of this research is to determine whether coastal development on Dauphin Island has influenced its shoreline dynamics, both coast side and bay side, through a comparison to two neighboring undeveloped islands: Horn and Petit Bois. Dauphin Island was selected because it is the only barrier island in the Alabama-Mississippi chain that is road-accessible and extensively developed with residential and commercial structures, making it an ideal case for assessing the geomorphic consequences of human disturbance. We hypothesize that shoreline retreat and erosion on the coast side of Dauphin Island, particularly in developed zones, are significantly greater than those observed on the undeveloped control islands. Accordingly, the research goal is to explicitly evaluate the extent to which development pressure alters shoreline dynamics by contrasting Dauphin Island with the more natural conditions of Horn and Petit Bois. By quantifying and comparing shoreline change metrics across developed and undisturbed systems, this study offers new empirical insights into the long-term impacts of human development on barrier island resilience, data that are crucial for informing sustainable coastal planning and climate adaptation strategies.

2. Research method

Of the three barrier islands located on the Alabama-Mississippi border, only Dauphin Island is accessible by road and developed with vacation homes and retail establishments. Continuous settlement of Dauphin Island dates back to 1701, but widespread modern development accelerated after Hurricane Frederic in 1979. By 2000, approximately 55 % of single-family lots were developed, leading to substantial alterations of native dune vegetation and sediment dynamics (Morton, 2008; U.S. Geological Survey, 2020).

In contrast, Petit Bois and Horn Islands are accessible solely by boat, with only small abandoned human-made structures on Horn. These islands retain intact natural dune systems, salt marshes, and maritime forests, offering a critical habitat for migratory birds, wildlife, and native plant communities (Guy, 2015b; Guy, 2015c). Horn Island features a complex mosaic of habitats, including dunes, swales, interior lagoons, and forested areas, while Petit Bois Island consists largely of dynamic beach and marsh systems. Both islands are under federal protection, with Horn Island included in the Gulf Islands National Seashore registry. These two islands retain natural dune systems and unique ecologies and serve as habitats for wildlife and migratory birds, as well as the occasional site of recreational activities such as fishing (Feagin et al., 2015; Morton, 2008). Unlike Dauphin Island, these undeveloped islands have not experienced infrastructure-induced sediment disruption, allowing them to maintain greater shoreline stability despite exposure to similar climatic forces (U.S. Geological Survey, 2007; Smith et al., 2018).

The research objective was to compare shoreline change patterns and rates of erosion and deposition between Dauphin Island and the comparison group, in order to assess any consistency or disparity in shoreline evolution. To answer this question, this study employed transect analysis to track shoreline changes over time, focusing on both the direction and rate of change. Given that shoreline changes vary even along sections of the same island due to complex interactions among currents, structures, and materials, transect analysis offered a practical approach to effectively capturing these variations (Han, 2021).

2.1. Research design

DSAS is an ArcMap extension designed for statistical shoreline analysis. It compiles shoreline polylines from different dates, generating transects that extend across the shoreline based on a user-defined baseline. In this study, the baseline was placed landward and approximately parallel to the general orientation of the shoreline to ensure that all transects intersected the shoreline perpendicularly. This approach aligns with DSAS best practices and helps minimize angle-induced distortion in shoreline change measurements (Himmelstoss et al., 2018).

This study followed a structured five-step process to analyze shoreline dynamics (see Fig. 2). Historical shoreline data from 1940 to 2015 were first compiled for both the coast and bay sides to capture long-term geomorphic trends under varying climatic and anthropogenic influences. The shorelines were then standardized and digitized into polylines to ensure spatial consistency, which was critical for comparing multiple datasets of different origins and resolutions. Using the earliest available shoreline as a baseline (1940 for Dauphin and 1984 for Petit Bois and Horn), DSAS projected transects perpendicular to the shoreline, enabling systematic measurement of change along comparable cross-sections. From these transects, key shoreline change metrics were calculated to quantify both the magnitude and direction of shoreline adjustments. Finally, these outputs were visualized in maps and scatterplots, allowing interpretation of how erosion, deposition, and island morphology have evolved over time and what ecological implications these changes may hold (Himmelstoss et al., 2018).

For this study, a baseline was created for each island's coast and bay sides using the earliest available shoreline from each dataset: 1940 for Dauphin Island and 1984 for both Petit Bois and Horn Islands. A new feature class was generated and a 50 m buffer created around the selected baseline. This interval was selected to provide sufficient resolution for capturing localized shoreline variability while maintaining computational efficiency across the large dataset. This buffer allows DSAS to systematically cast transects that intersect the shoreline perpendicularly, minimizing edge effects and ensuring consistent spatial analysis across the time series (Himmelstoss et al., 2018).

Points of intersection between the transects and shoreline provide observations of positive or negative distance values over time, which are then averaged to create predictive models capturing rates and distances of shoreline change. In the present research, these models yielded information on erosion and deposition rates, aiding the analysis of shoreline trends for both the bay and coastal sides of each island.

2.2. Data collection

DSAS utilizes satellite imagery and other geospatial data sources to generate historical shoreline vectors through a structured, GIS-based workflow (Himmelstoss et al., 2018). These shorelines are derived from a variety of sources, including satellite imagery (e.g., Landsat), georeferenced historical maps, GPS field surveys, aerial photographs, and high-resolution LiDAR data. Each dataset presents inherent variability in spatial resolution and positional accuracy; for instance, Landsat imagery offers 30-m resolution, whereas LiDAR datasets can achieve sub-meter precision (see Table 1). To manage such heterogeneity, DSAS requires all shoreline features to be integrated into a single feature class within a geodatabase, with each shoreline line assigned a specific date and source information (U.S. Geological Survey, 2023, p. 10).

In this study, shorelines were derived from both the High-Water Line (HWL), primarily interpreted from aerial and satellite imagery, and the Mean-High Water (MHW). HWL is widely used, but can be influenced by short-term environmental conditions such as storm surges, wind-driven tides, or seasonal vegetation, potentially introducing higher variability and landward bias in comparison to MHW (Morton, 2008). In contrast, MHW is a tidally referenced proxy that generally provides more consistent and repeatable measurements across time, though it requires

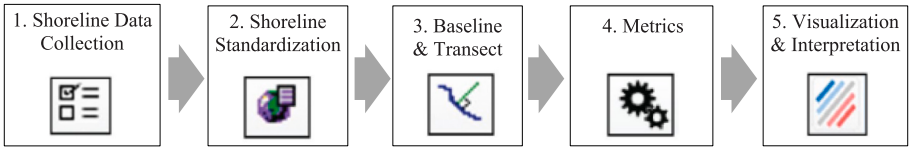

Fig. 2. DSAS workflow (revised based on Himmelstoss et al., 2018, p. 19): This research followed a five-step process and used the DSAS research framework to analyze shoreline dynamics.

Table 1
Shoreline Dataset Sources DSAS integrates various satellite imagery and provides historical shoreline vectors through a structured, GIS-based workflow (Himmelstoss et al., 2018).

Dataset Year	Data Source Type	Source / Provider	Spatial Resolution	Shoreline Proxy	Positional Uncertainty (m)
1985	Aerial Photograph	USGS National Map	~1–3 m	HWL	10
1998	Satellite Imagery	Landsat 5 (USGS)	30 m	HWL	10
2005	LiDAR	NOAA Digital Coast	<1 m	MHW	2
2010	GPS Shoreline Survey	Alabama Dept. of Env. Mgt	Sub-meter	MHW	3
2015	Satellite Imagery	Landsat 8 (USGS)	15 m (panchromatic)	HWL	8

higher-resolution data acquisition (e.g., LiDAR).

All shoreline datasets were projected into a common coordinate system (meters) and include required attribute fields such as date, uncertainty, and shoreline type. Before merging aerial, satellite, and LiDAR-derived shorelines, geometric distortions should be corrected and a consistent tidal datum (e.g., MHW) applied for cross-comparison (Himmelstoss et al., 2018, p.19–46). LiDAR-derived shorelines are generated from elevation profiles referenced to the operational MHW, with associated errors, proxy-datum biases, and water-level uncertainties explicitly recorded (Himmelstoss et al., 2018, p.8–19). These uncertainty values are then propagated into weighted regressions and confidence intervals, improving the reliability of shoreline change statistics (Himmelstoss et al., 2021, p.28).

To account for positional uncertainty inherent in shoreline data, we applied a default uncertainty value of ±10 m for all shoreline positions, as recommended when metadata is incomplete or variable (Himmelstoss et al., 2021, p. 28). In DSAS, these uncertainty values propagate into the shoreline change rate calculation, for instance LRR, via weighted regression and confidence interval estimation (Himmelstoss et al., 2021). The DSAS User Guide explains that when shoreline datasets lack complete metadata, a default value of 10 m is provided as the approximate average positional uncertainty across aerial, satellite, and LiDAR-derived shorelines used in USGS regional shoreline change reports (U.S. Geological Survey, 2023, p.25). While users are encouraged to calculate dataset-specific uncertainties when possible, applying a uniform 10 m value ensures methodological consistency and minimizes bias in comparative analyses across islands.

The initial set of shorelines for Dauphin Island was calculated using two shoreline proxy datasets from 1985 to 2015: mean high water shorelines, which represented the average height of hide tides over a defined period and were generated from 14 LiDAR datasets, and wet-dry line shorelines, which delineated the visible boundary between moist and dry areas as interpreted from imagery; these were digitized from 10 sets of georeferenced aerial images (Henderson et al., 2017). Shoreline datasets for Petit Bois and Horn Islands were extracted from satellite imagery dating from 1984 to 2015 (Guy, 2015b, 2015c). These datasets were acquired in digital format from the USGS Earth Resources Observation and Science Center Global Visualization Viewer (Guy, 2015a).

Petit Bois and Horn Islands contained multiple shoreline data entries within the same year. To generate a single observation per year, all datasets for each target year were standardized and reprocessed accordingly. (Himmelstoss et al., 2018). The analysis employed transects spaced at intervals of 50 m along the coast and bay sides of each island. A total of 618 transect lines were generated for this research.

2.3. Shoreline change statistics

DSAS provides three key statistical analyses to examine shoreline change, including NSM, SCE, and LRR. These analyses are reported in units of meters for distances and meters/year for rates of change, which collectively help illustrate shoreline morphological patterns by capturing movement direction, magnitude, and rate of change. Fig. 3 illustrates the detailed concepts related to shoreline change, which were generated from DSAS, as well as the concepts of NSM, SCE, and LRR, with the example of a transect. In the figure, 12 years of shorelines (in multiple colors) measured from 1963 to 2005 met a single transect (a gray line perpendicular to the baseline towards the shoreline). The shoreline changes were measured in terms of the distances from the baseline (a black line) for further analysis (see Fig. 3).

A. *Net Shoreline Movement (NSM):* NSM is the distance between the earliest and most recent shorelines along each transect. In the example presented in Fig. 4, NSM is the distance from the red line (1936) to the magenta line (2005). Positive NSM values indicate deposition, while negative values indicate erosion. This was used here to identify trends in erosion and deposition, allowing for comparisons between Dauphin Island and the control islands. In the present research, NSM was used to determine: 1) the presence of both erosion and deposition along the shoreline, 2) ratio of erosion to deposition, and 3) overall movement direction of coast- and bayside shorelines.
B. *Shoreline Change Envelope (SCE):* SCE measures the greatest distance between all shorelines intersecting a transect, regardless of direction. Thus, with the Fig. 4 example, 1963 to 2004 shows the greatest distance of shoreline changes between 1936 and 2005. This metric was useful for assessing fluctuations in shoreline change on both the coast and bay sides, focusing on the magnitude of change. SCE helped compare shoreline fluctuation trends between islands by analyzing the maximum shoreline movement for each segment.
C. *Linear Rate of Regression (LRR):* LRR calculates the rate of shoreline movement using the slope of a least squares regression line. It was employed to determine whether shoreline change rates were consistent or variable between the islands. Higher rates or a dominance of erosion or deposition would indicate accelerated shoreline change, while consistency suggests stability. LRR values are reported in $m \cdot yr^{-1}$ and provide an understanding of the directional rate of shoreline change.

In this study, a 90 % confidence interval was applied to quantify the uncertainty for the statistical analysis. This interval was calculated by multiplying the standard error of the slope by the critical value of a two-

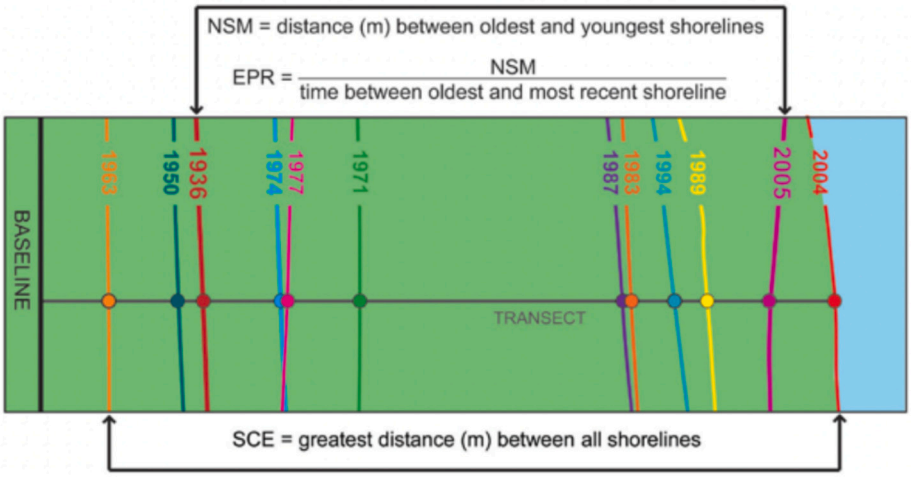

Fig. 3. Illustration of NSM and SCE (Himmelstoss et al., 2018, p. 48).

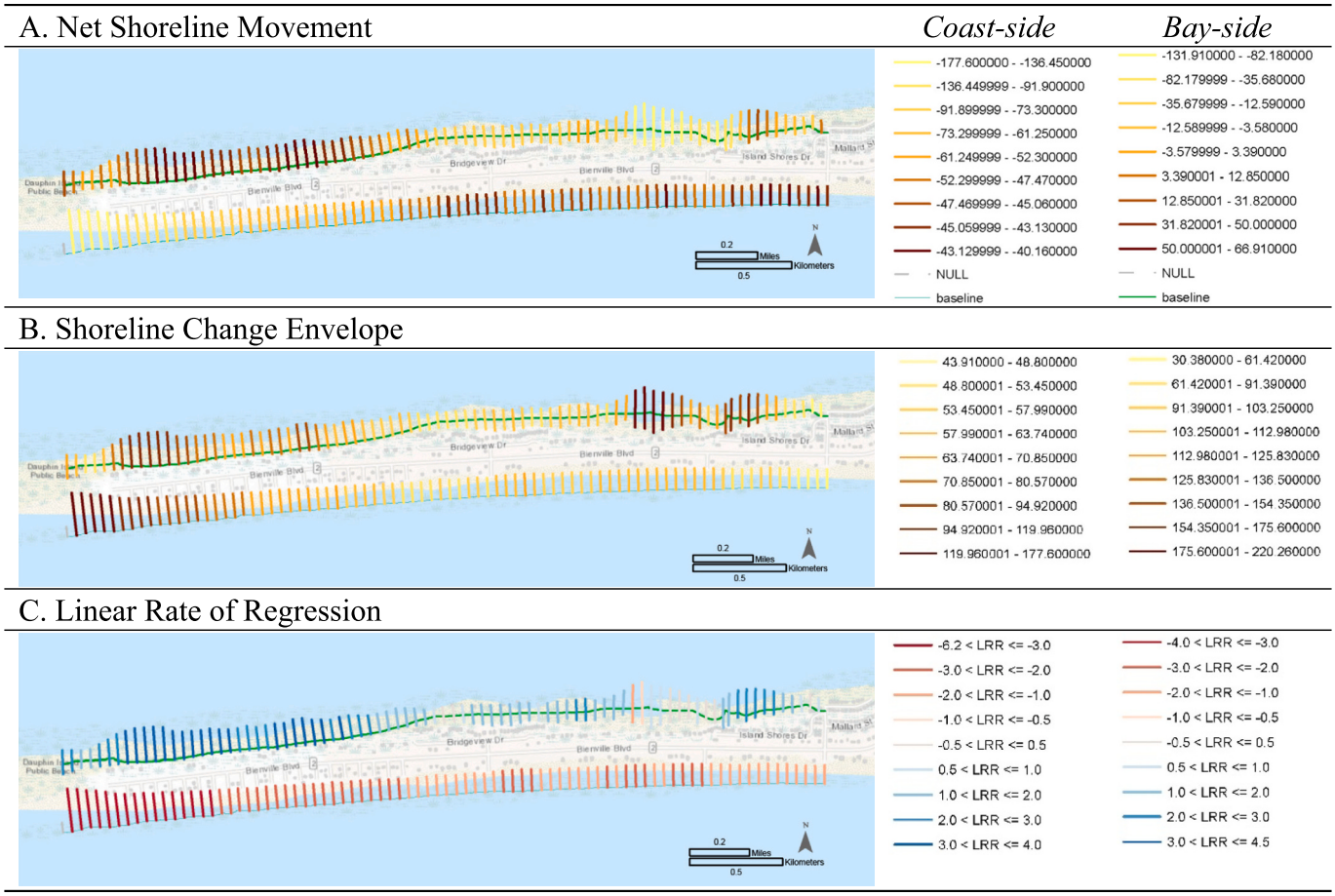

Fig. 4. Dauphin Island transects: The following figures represent the NSM, SCE, and LRR results for the Dauphin Island transects. The colors in the figure below represent the direction and magnitude of shoreline movement, with red indicating erosion and green/blue indicating deposition. (For interpretation of the references to colour in this figure legend, the reader is referred to the web version of this article.)

tailed t-distribution at the 90 % confidence level, producing a statistical range within which the true rate of shoreline change was expected to fall with 90 % certainty. This approach allowed for a deeper understanding of shoreline trends and improved the model's accuracy (Himmelstoss et al., 2018).

3. Results

3.1. Island shoreline change analysis

With 82 on the coast side and 83 on the bay side, a total 165 transects of Dauphin Island were analyzed. All coastal transects exhibited erosion

patterns, while the bayside transects were almost evenly split between erosion (47 %) and deposition (53 %). However, on average, net deposition was observed on the bay side, suggesting that Dauphin Island is shifting towards the mainland. The magnitude of shoreline change was approximately 1.8 times greater on the bay side than on the coast side (see Fig. 4). The NSM indicated 100 % erosion on the coast side and mixed erosion-deposition patterns on the bay side. The SCE showed the maximum spatial variability in shoreline position, with more pronounced inland movement on the bay side. The LRR highlighted a consistent trend of chronic coast-side erosion and bay-side accretion, suggesting net island migration towards the mainland.

In terms of NSM (see Table 2), all coast-side transects (100 %) showed an average of 62.26 m of erosion and no deposition. The maximum erosion observed was 177.6 m, indicating significant shoreline retreat in certain areas. These data reveal a consistent erosional pattern characteristic of chronic coastal retreat. Conversely, on the bay side, 39 transects (46.99 %) showed erosion, while 44 transects (53.01 %) exhibited deposition. The average changes were 35.15 m for erosion and 28.59 m for deposition. The maximum erosion distance was 131.91 m, while the average erosional distance was 35.15 m. For deposition, the maximum distance recorded was 66.91 m, with an average of 28.59 m. Based on the number of transects and average distances, a net deposition of approximately 121.56 m was observed on the bay side.

Over the 30-year period, the developed areas of Dauphin Island showed an average coastal erosion of 62.26 m along the coast side, while the island migrated an average of 121.56 m towards the mainland along the bay side. The SCE analysis of Dauphin Island yielded similar results to that of the NSM. On the coast side, between 1985 and 2015, the maximum shoreline change was 177.6 m, with a minimum of 2.26 m. The average shoreline change was 69.2 m. Although the SCE did not indicate the direction of change, its similarity to the NSM average of 62.26 m suggests an erosional trend. For the bay side, the maximum shoreline change was 220.26 m, while the minimum change was 30.38 m, approximately 75 % greater than the change on the coast side. The average SCE on the bay side was 121.56 m, which matched the NSM value, indicating ongoing deposition towards the mainland over the past 30 years.

The LRR analysis for Dauphin Island showed that all coast-side transects displayed negative values, indicating erosion across 100 % of the transects. The maximum rate of change was –6.19 m·yr^{-1}, with an average rate of –2.49 m·yr^{-1}. On the bay side, an average deposition rate of 2.02 m·yr^{-1}was observed, though a mixture of erosional and depositional changes was noted. Among the 83 transects, three (3.61 %) exhibited erosion, with a maximum rate of –1.3 m·yr^{-1} and average rate of –0.66 m·yr^{-1}. The remaining 80 transects (96.39 %) experienced deposition, with a maximum rate of 4.43 m·yr^{-1} and average rate of 2.12 m·yr^{-1}.

Overall, the island's thickness increased, while its position shifted towards the mainland. In summary, the coast side appears to be eroding at a rate of –2.49 m·yr^{-1}, while the bay side is experiencing deposition at a rate of 2.02 m·yr^{-1}. The island is shifting towards the mainland at an average rate of 2.26 m·yr^{-1} (the combined average of 2.49 and 2.02 m·yr^{-1}), with a reduction in island thickness by approximately 0.47 m·yr^{-1}.

On Petit Bois Island there were 240 transects, 122 coast side and 118 bayside. The overall results indicated significant net erosion on both the coast-side and bayside shorelines, with varying degrees of fluctuation between erosion and deposition. The NSM showed a higher concentration of erosion on both the coast and bay sides, with the bay side exhibiting nearly complete erosion. The SCE indicated moderate spatial variability, especially on the coast side. The LRR results revealed consistent but slightly less severe rates of shoreline retreat on both sides, as compared to Dauphin Island. The coast side demonstrated greater variability, with a fluctuating balance between erosion and deposition, while the bay side was showing signs of chronic erosion and minimal depositional activity (see Fig. 5).

Regarding the NSM (see Table 3), the coast side of Petit Bois Island experienced a net erosion of 34.3 m. On average, the erosional distance was −64.3 m, while the depositional distance averaged 40.87 m. The total number of erosional transects was 87, as compared to 35 depositional transects. These results suggest a fluctuating dynamic between erosion and deposition, though the overall net trend was erosion. Specifically, the ratio of erosional to depositional movement was approximately 71.3 % to 28.7 %, indicating that erosion predominated along the coast side.

On the bay side, the NSM showed a more severe pattern of erosion, with a net erosional distance of −53.86 m. The average erosional distance was −54.44 m, while the average depositional distance was minimal: 2.04 m. The number of erosional transects was 117, and there was only one depositional transect. These findings indicate a strong net erosive pattern along the bay side and very limited depositional activity, suggesting that this shoreline was experiencing chronic erosion.

The SCE results demonstrated an average shoreline change of 118.34 m along the coast side and 68.1 m along the bay side. The maximum shoreline change distance on the coast side was 206.69 m, while the bay side experienced a maximum change of 129.38 m. Comparatively, the coast-side shoreline of Petit Bois Island showed significantly greater fluctuation in movement than did the bay side, with approximately 74 % less change occurring along the bay side. This pattern contrasts with what was observed on Dauphin Island, where the magnitude of shoreline change displayed a different ratio between coast-side and bayside fluctuations.

The LRR analysis for the coast-side shoreline of Petit Bois revealed an average rate of erosion of −2.49 m·yr^{-1} and average depositional rate of 0.32 m·yr^{-1}. Overall, the net rate of change was −1.86 m·yr^{-1}, suggesting a net erosional movement pattern. The ratio of erosional to depositional transects was 95 to 25, reinforcing the overall erosional trend. It is important to note that although the average erosion rate of −1.86 m·yr^{-1} was relatively high, it remained lower than the rate observed for Dauphin Island's coast, which was −2.49 m·yr^{-1}.

A total of 213 transects for Horn island were analyzed, 106 on the coast side and 107 on the bay side. The key findings highlight considerable variability in shoreline movement, with both erosion and deposition occurring across different areas of the island (see Fig. 6). The NSM showed relatively balanced erosion and accretion patterns on the coast side, while the bay side was dominated by erosion. The SCE indicated moderate shoreline fluctuations along the coast and minimal change on the bay side. The LRR results reflected a low and stable rate of shoreline change, with a minor net retreat suggesting Horn Island's strong sediment retention and minimal inland migration.

Table 2
Dauphin Island Shoreline Analysis: A shoreline change analysis showed 100 % erosion on the coast side, with an average loss of 62.26 m and no deposition. In contrast, the bay side experienced 53 % deposition and 47 % erosion, resulting in a net inland migration of 121.56 m.

	Coast-side	Bay-side
Summary		
Total no. transects (ea)	82	83
Average NSM distance (m)	−62.26	121.56
Average SCE distance (m)	69.26	121.56
Average LRR rate (m·yr^{-1})	−2.49	2.02
Erosion		
Total no. erosion transects (ea)	82	39
Percent of erosion transects (%)	100	46.99
Maximum erosion distance (m)	−177.6	−131.9
Average erosion distance (m)	−62.26	−35.15
Average erosion rate (m·yr^{-1})	−2.49	−0.66
Accretion		
Total no. accretion transects (ea)	0	44
Percent of accretion transects (%)	0	53.01
Max accretion distance (m)	0	66.91
Average accretion distance (m)	0	28.59
Average accretion rate (m·yr^{-1})	0	2.12

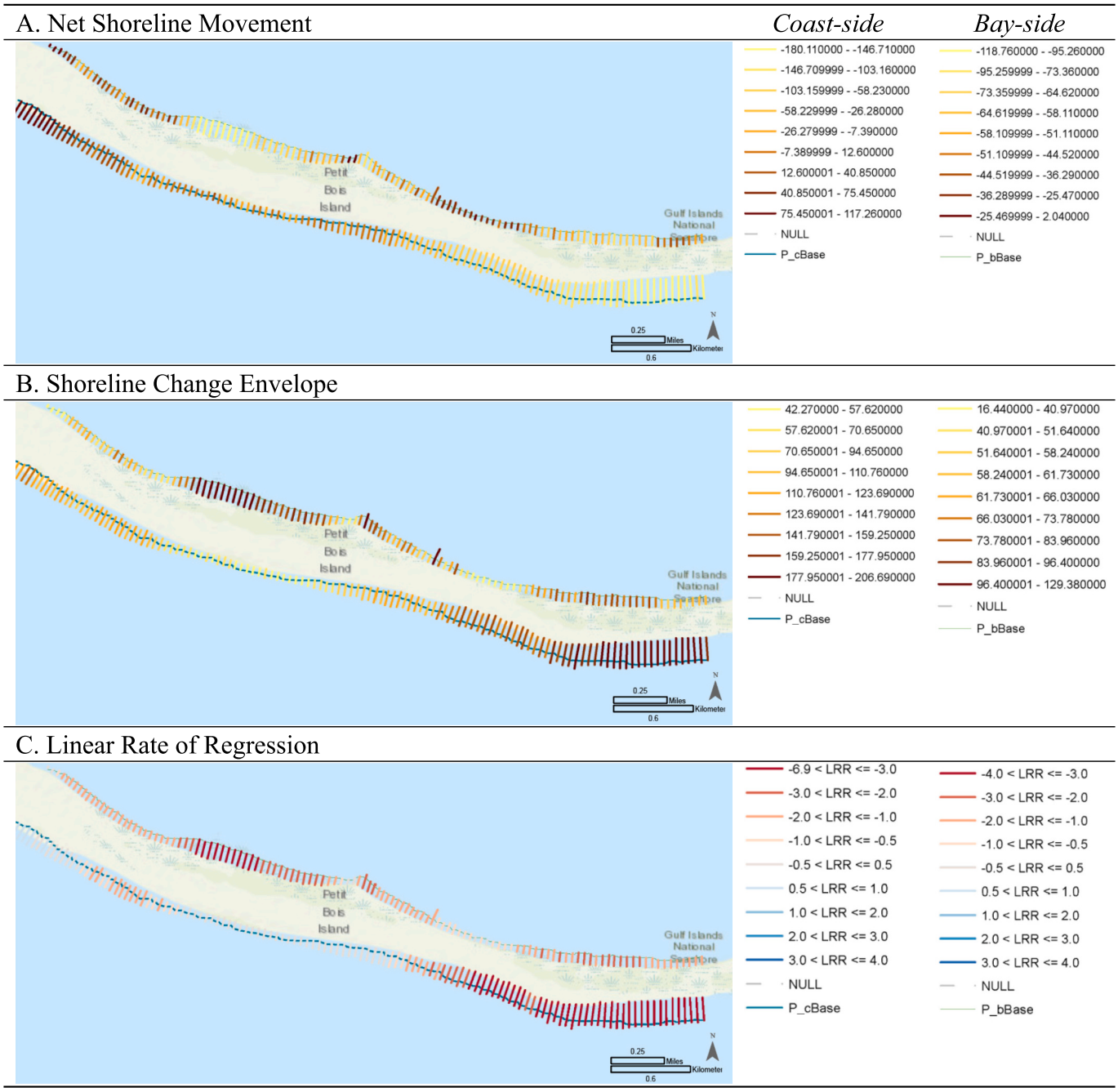

Fig. 5. Petit Bois Island Transects: The following figures represent the NSM, SCE, and LRR results for Petit Bois Island's transects.

Horn Island's NSM (see Table 4) results showed net erosion for both the coast-side and bayside areas. The coast side exhibited an average net erosion of −2.56 m, with individual transects indicating a mix of erosion and deposition (average erosion at −57.99 m and deposition at 64.43 m). Erosional transects made up 61.48 % of the total (58 out of 106). The fluctuation between erosion and deposition indicated a lack of consistent directional movement, resulting in moderate net erosion for the coast side.

For the bay side, the average net erosion was −22.76 m. The bayside transects displayed a significant imbalance between erosion and deposition, with 89.72 % showing deposition and only 10.28 % showing erosion. The average shoreline movement was −26.46 m for erosion and 9.53 m for deposition, suggesting fluctuating shoreline dynamics, but with an overall net erosional trend.

Horn Island's SCE results displayed an average shoreline change of 113.11 m on the coast side and 41.41 m on the bay side. The maximum shoreline change distance recorded was 183.91 m for the coast side and 99.25 m for the bay side. This indicates that the bay side experienced significantly less change, with shoreline changes being over three times smaller in magnitude as compared to the coast side.

The LRR results showed an average shoreline change rate of −2.12 $m \cdot yr^{-1}$on the coast side and − 0.69 $m \cdot yr^{-1}$on the bay side. The average deposition rate for the coast side was 1.9 $m \cdot yr^{-1}$, with a net average of −0.53 $m \cdot yr^{-1}$. The coast side exhibited a relatively balanced ratio of erosional to depositional transects, with 48 transects indicating erosion and 58 showing deposition.

Following the shoreline change analysis of each island, a statistical test was conducted using coast-side transects from all three islands to evaluate whether observed differences in shoreline dynamics were statistically significant and to identify which metrics best distinguished the

Table 3
Petit Bois Island Shoreline Analysis A shoreline change analysis showed that 71 % of coast-side transects and 99 % of bayside transects experienced erosion, indicating an overall shoreline retreat on both fronts with limited accretion, suggesting declining sediment stability across the island.

	Coast-side	Bay-side
Summary		
Total no. transects (ea)	122	118
Average NSM distance (m)	−34.13	−53.86
Average SCE distance (m)	118.34	68.1
Average LRR rate (m·yr^{-1})	−1.86	−1.76
Erosion		
Total no. erosion transects (ea)	87	117
Percent of erosion transects (%)	71.31	99.15
Maximum erosion distance (m)	−180.11	−118.76
Average erosion distance (m)	−64.3	−54.44
Average erosion rate (m·yr^{-1})	−2.42	−1.78
Accretion		
Total no. accretion transects (ea)	35	1
Percent of accretion transects (%)	28.69	0.85
Max accretion distance (m)	117.26	2.04
Average accretion distance (m)	40.87	2.04
Average accretion rate (m·yr^{-1})	0.32	0

Table 4
Horn Island Shoreline Analysis**:** The following figures represent the NSM, SCE, and LRR results for Horn Island's transects.

	Coast-side	Bay-side
Summary		
Total no. transects (ea)	106	107
Average NSM distance (m)	−2.56	−22.76
Average SCE distance (m)	111.11	41.41
Average LRR rate (m·yr^{-1})	−0.53	−0.69
Erosion		
Total no. erosion transects (ea)	58	96
Percent of erosion transects (%)	54.72	89.72
Maximum erosion distance (m)	−115.48	−66.2
Average erosion distance (m)	−57.99	−26.46
Average erosion rate (m·yr^{-1})	−2.12	−0.8
Accretion		
Total no. accretion transects (ea)	48	11
Percent of accretion transects (%)	45.28	10.28
Max accretion distance (m)	127.93	16.25
Average accretion distance (m)	64.43	9.53
Average accretion rate (m·yr^{-1})	1.9	0.28

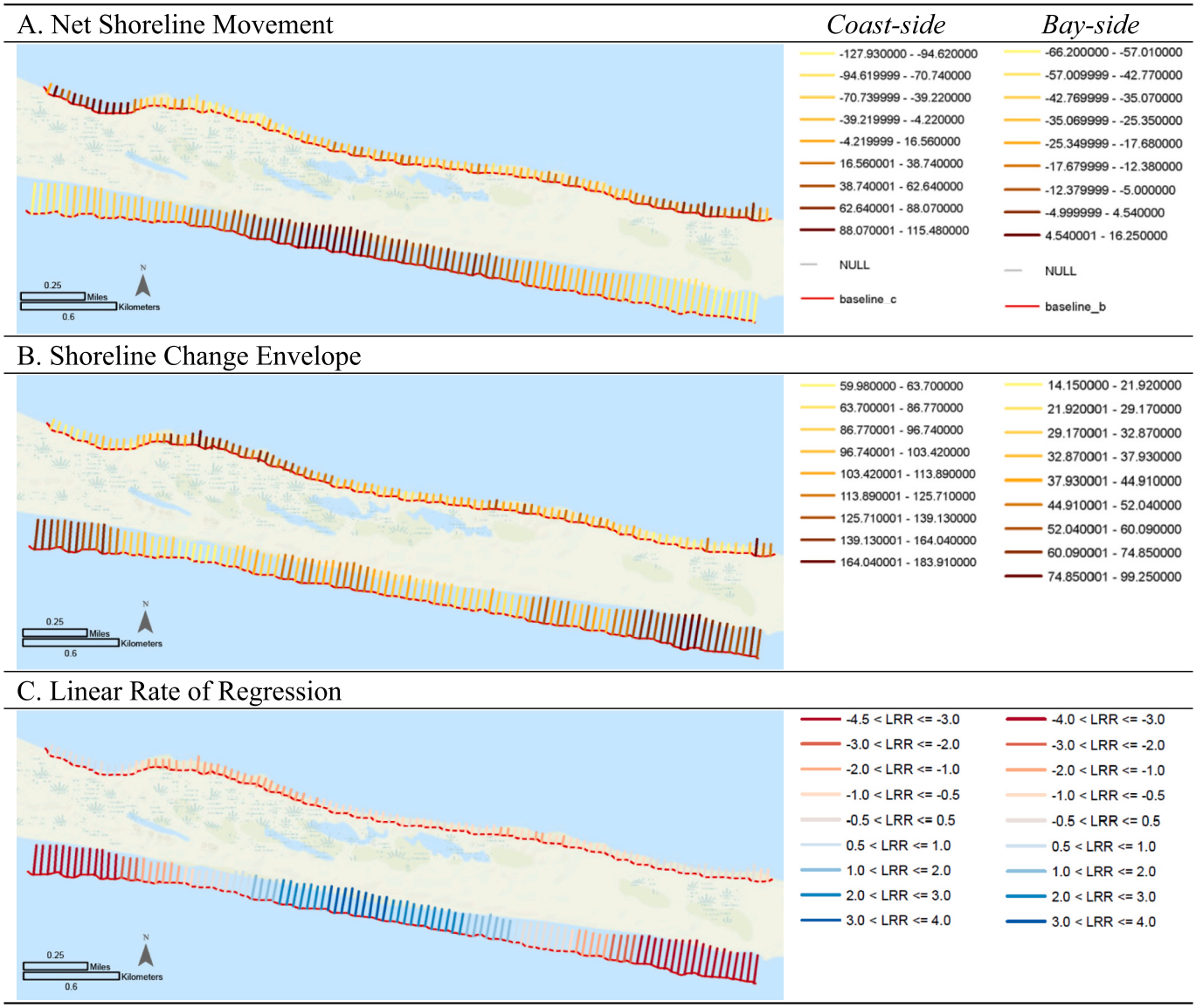

Fig. 6. Horn Island Transects: The following figures represent the NSM, SCE, and LRR results of Horn Island's transects.

islands from one another. A total of 310 coast-side transects were included in the analysis: 82 from Dauphin Island, 122 from Petit Bois Island, and 106 from Horn Island. Three raw measurements for each transect, NSM, SCE, and LRR, were used in a one-way analysis of variance (ANOVA), followed by post hoc comparisons using Tukey's HSD test.

The ANOVA results indicated statistically significant differences among the three islands across all three metrics (NSM: $F(2,310) = 11.18$, $p = 0.00002$; SCE: $F(2, 310) = 47.52$, $p < 0.0001$; LRR: $F(2, 310) = 5.91$, $p = 0.003$). Post hoc comparisons revealed that, for LRR, Dauphin Island differed significantly from Horn Island ($p = 0.0030$) but not from Petit Bois Island ($p = 0.8734$). In contrast, for NSM, Dauphin differed significantly from both Horn ($p = 0.0000$) and Petit Bois ($p = 0.0080$). For SCE, a significant difference was observed between Dauphin and Petit Bois ($p = 0.0000$), while the difference between Dauphin and Horn was not statistically significant ($p = 0.6178$). Additionally, Horn and Petit Bois differed significantly in LRR ($p = 0.0050$) and SCE ($p = 0.0000$), but not in NSM ($p = 0.1333$) (see Fig. 7).

These findings provide statistically grounded evidence that the spatial patterns of shoreline change on Dauphin Island are distinct from those observed on the adjacent undeveloped barrier islands. The most pronounced distinctions appear in the NSM and SCE metrics, which capture cumulative and episodic shoreline shifts over time.

4. Discussion

By integrating 30 years of historical shoreline data, this study confirms significant differences in shoreline change trends, especially on the

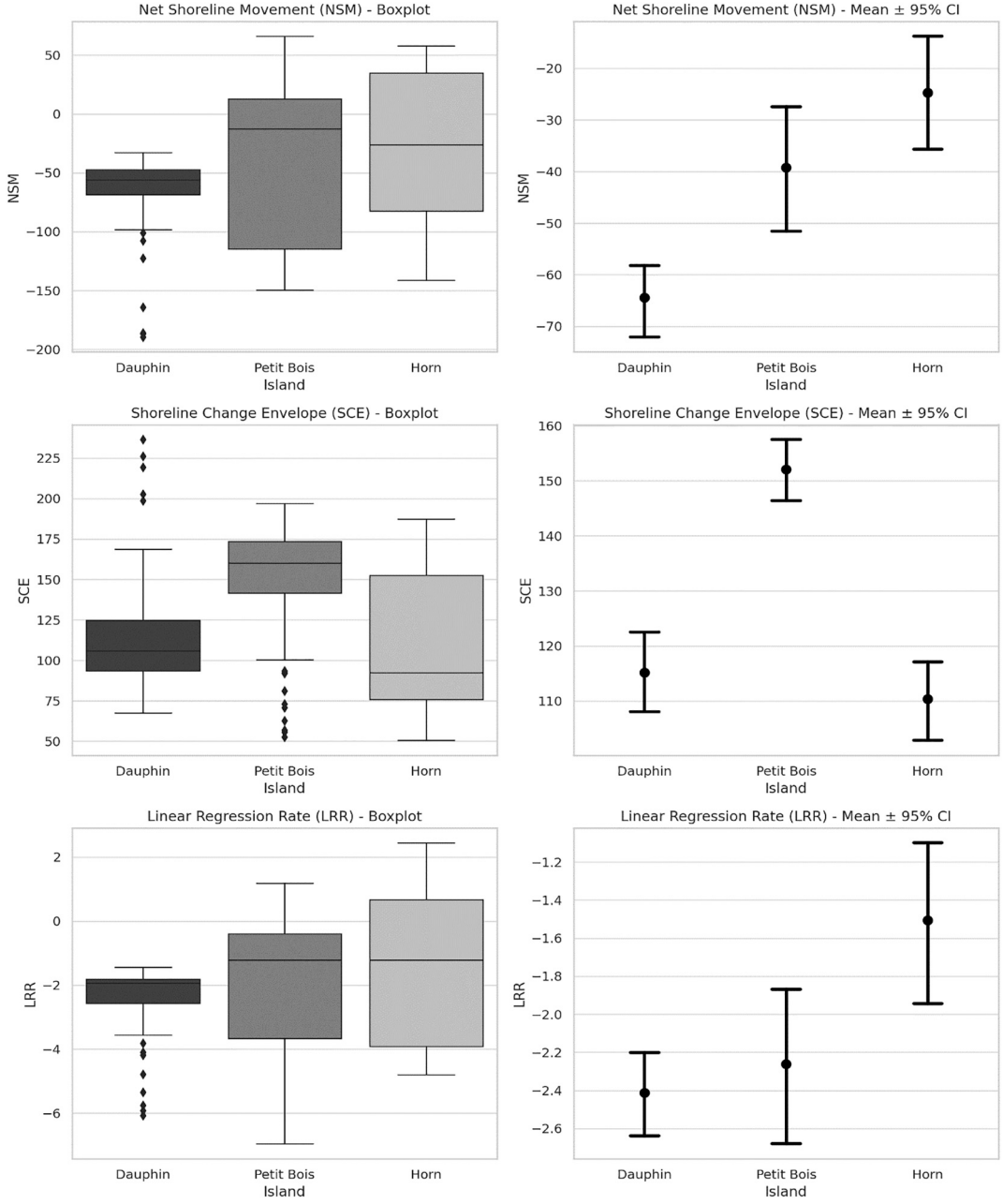

Fig. 7. ANOVA and Tukey HSD post hoc test results for shoreline change metrics. Boxplots (left) and mean ± 95 % confidence interval plots are shown for three shoreline-change metrics: top (NSM), middle (SCE), and bottom (LRR). The boxplots illustrate the spread and skewness of shoreline change measurements across transects, while the confidence interval plots emphasize differences in group means. Statistically significant differences were observed between islands for all metrics ($p < 0.05$) based on one-way ANOVA with Tukey HSD post hoc tests.

coast side of Dauphin Island where intensive development has occurred since the mid-20th century. The results support the hypothesis that Dauphin Island exhibits accelerated shoreline retreat compared to the relatively stable conditions of Horn and Petit Bois Islands. These findings reinforce the notion that anthropogenic disturbances can accelerate coastal degradation by disrupting sediment processes and altering the natural protective features of barrier islands.

The comparative analysis also aligns with global studies that document divergent shoreline trajectories under varying human pressures. For instance, extensive erosion on Sagar Island in West Bengal contrasts with predominantly accretional trends on Kerala's Vypin and Vallarpadam Islands, where port development has played a significant role (Chettiyam Thodi et al., 2023; Gopinath et al., 2023). Such comparisons highlight that the geomorphic contrasts observed between Dauphin and the undeveloped islands are consistent with broader patterns reported internationally.

In summary, this study provides new empirical evidence of how development pressure shapes barrier island dynamics, while also situating local findings within global contexts and acknowledging methodological constraints. These contributions underscore the importance of integrating natural dune and vegetation management into sustainable coastal planning and climate adaptation strategies.

4.1. Net shoreline movement (NSM)

The NSM results highlight distinct sedimentary behaviors across the three islands, reflecting both natural processes and varying levels of human disturbance. Dauphin Island exhibited the greatest instability, with pronounced coast-side erosion, significant bayside accretion, and evidence of inland migration. This imbalance suggests a breakdown of sediment feedback mechanisms that typically stabilize barrier islands, a condition strongly associated with vegetation loss and development pressure. Petit Bois Island showed more moderate dynamics: while erosion dominated, localized deposition indicated partial sediment redistribution, though the lack of bayside deposition suggests insufficient vegetative or dune structure to stabilize both margins. Horn Island, by contrast, maintained the most balanced pattern, with near-equilibrium sediment exchanges and minimal inland migration, reflecting the stabilizing role of intact vegetation and limited human interference. Overall, the NSM analysis supports the interpretation that development-driven disruptions to natural sediment feedback loops accelerate geomorphic instability.

4.2. Shoreline change envelope (SCE)

The SCE analysis, which captures the full range of shoreline displacement, revealed contrasting resilience among the islands. Dauphin Island experienced the largest magnitude of shoreline movement, particularly on the bay side, suggesting intensified inland sediment transfer due to degraded dune systems and repeated overwash. Petit Bois Island showed moderate shoreline variability, greater on the coast side than the bay side, indicating some functional cross-shore sediment exchange despite partial disturbance. Horn Island displayed minimal SCE values overall, consistent with a stable sediment-binding system supported by vegetation and natural dune morphology. Taken together, the SCE results reinforce the broader conclusion that compromised coast-side stabilization systems, as observed on Dauphin Island, amplify shoreline change across the island, whereas intact systems, as on Horn Island, sustain long-term geomorphic resilience.

Taken together, the SCE results reinforce the hypothesis that barrier island stability is closely linked to the functionality of coast-side sediment retention systems. Where these systems are compromised—as seen on Dauphin Island—shoreline movement intensifies and propagates across the island. Conversely, undeveloped or minimally disturbed islands like Horn Island demonstrate higher resilience due to intact sediment feedback loops and ecological structures. These findings support broader arguments for integrating vegetative management and dune conservation into shoreline protection strategies under ongoing climate stressors (Durán and Moore, 2013; Feagin et al., 2015; Hanley et al., 2014).

4.3. Linear rate of regression (LRR)

The LRR results further underscore the role of human disturbance in shaping long-term shoreline trajectories. Dauphin Island exhibited chronic coast-side erosion and bayside accretion, signaling ongoing inland sediment migration and a disrupted equilibrium. Petit Bois Island showed somewhat lower erosion rates and limited depositional activity, suggesting partially functioning but weakened sediment feedback. Horn Island maintained low and balanced rates of change, reflecting geomorphic stability under minimal anthropogenic pressure. Importantly, while ANOVA confirmed statistically significant differences among the three islands, the LRR trends emphasize that development not only alters the rate but also the spatial balance of shoreline change. In summary, the LRR findings support the hypothesis that shoreline stability is closely tied to natural sediment feedback mechanisms and the presence of vegetative stabilization features. Dauphin Island's disrupted patterns and elevated shoreline activity highlight the geomorphic consequences of human development. In contrast, the lower and more balanced rates observed on Petit Bois and Horn Islands illustrate how intact dune systems and limited disturbance can sustain long-term shoreline equilibrium.

5. Conclusion

This research empirically demonstrates the differential response of developed and undeveloped barrier islands to environmental and anthropogenic pressures. It provides quantitative evidence for guiding restoration and land-use policies and contributes to a growing body of knowledge on the interplay between human development and coastal geomorphology.

The results confirm the hypothesis that shoreline change on Dauphin Island differs significantly from the relatively stable patterns observed on the undeveloped islands. Dauphin Island exhibited persistent shoreline retreat on the coast side and significant inland sediment migration on the bay side, suggesting chronic geomorphic instability. In contrast, Petit Bois and Horn Islands demonstrated a more balanced and self-regulating dynamic between erosion and deposition. These findings indicate that human development has disrupted natural sediment flow and weakened the island's capacity to recover from high-energy events such as storms and overwash.

Importantly, these spatial patterns have tangible ecological and environmental implications. The loss of vegetated dunes and increased shoreline retreat are not merely geomorphic shifts but represent degradation of essential coastal habitats (Durán and Moore, 2013; Feagin et al., 2015). These ecosystem-level effects align with similar findings in other barrier island systems such as the Outer Banks and Galveston Island, where development-induced dune loss has been linked to habitat fragmentation and increased storm surge exposure (Hanley et al., 2014; Stallins, 2005).

Beyond the ecological context, this study offers valuable insight for sustainable coastal planning and policy. The contrast between developed and undeveloped islands underscores the importance of maintaining vegetative cover and dune integrity as a nature-based solution to shoreline protection. Our findings reinforce the recommendations of the Alabama Coastal Area Management Program and State Expenditure Plan, which advocate for dune restoration, habitat conservation, and strategic development limitations in erosion-prone coastal zones (Alabama Department of Environmental Management (ADEM), 2022; Dauphin Island Sea Lab and Alabama Department of Conservation and Natural Resources (DCNR), 2018).Furthermore, the historical shoreline data here can serve as analytic tools for identifying high-risk areas,

guiding zoning, setback policies, and soft stabilization measures such as native vegetation planting and controlled dune rebuilding.

Despite the strength of these findings, this study has several limitations that should be acknowledged. It is constrained by reliance on remote sensing datasets and the application of a uniform ±10 m uncertainty value across all shorelines. While this approach follows DSAS guidelines and enables comparability, field validation of vegetation dynamics and higher-resolution uncertainty testing (e.g., sensitivity analyses) would strengthen future research. Accordingly, this study highlights the need for further research. Incorporating diverse higher-resolution datasets, conducting field-based investigations, and applying non-linear modeling of shoreline change would allow for a more precise assessment of shoreline dynamics across the three islands. By addressing these limitations, subsequent studies could provide a more comprehensive understanding of how development pressures and natural processes jointly shape the resilience of barrier islands under changing climate conditions.

To provide implementation strategies and prioritization, this study recommends a phased approach. First, dune restoration should be considered the most urgent priority, focusing on re-establishing native vegetation and sediment re-accumulation to strengthen natural buffer functions in erosion-prone areas. Second, zoning and setback regulations should be strategically applied, particularly in zones with high shoreline retreat rates. These policies should emphasize managed retreat and relocation of existing developments rather than permitting new construction in vulnerable areas. Finally, soft stabilization measures, including vegetative sand trapping and the minimization of hard infrastructure, should be implemented, emphasizing nature-based solutions over engineered interventions. Prioritizing these strategies not only enhances resilience to sea-level rise and intensified storm events under climate change but also offers cost-effective and ecologically sustainable pathways for long-term coastal management.

We hope that this research can provide crucial insights to policy-makers and practitioners in coastal management and planning who are working towards integrated, climate-resilient, and ecologically sound shoreline management.

Author contribution

Dr. Han contributed to the research design, data collection, analysis, and writing. Dr. Schauwecker contributed to the research design and manuscript review.

Declaration of generative AI in scientific writing

We have nothing to declare.

Funding sources

This work was partially supported by the National Academies of Sciences, Engineering, and Medicine, Gulf Research Program.

Declaration of competing interest

The authors declare that they have no known competing financial interests or personal relationships that could have appeared to influence the work reported in this paper.

Acknowledgments

We would like to express our gratitude to Walter Hogue, a Master of Landscape Architecture student at Mississippi State University, for his valuable assistance and collaboration during the initial stages of this research. His contributions to data collection and preliminary analysis were instrumental in laying the foundation for this study.

Data availability

The data and analytical materials supporting this research have been uploaded to the open-access repository Zenodo (https://doi.org/10.5281/zenodo.16856827). They are publicly available to ensure the reproducibility of the research and to comply with journal requirements for data transparency.

References

Alabama Department of Environmental Management (ADEM), 2022. Alabama Coastal Area Management Program (ACAMP). https://adem.alabama.gov/coastal.

Bilskie, M.V., Hagen, S.C., Alizad, K., Medeiros, S.C., Passeri, D.L., Needham, H.F., Cox, A., 2016. Dynamic simulation and numerical analysis of hurricane storm surge under sea level rise with geomorphologic changes along the northern Gulf of Mexico. Earth's Future 4 (5), 177–193. https://doi.org/10.1002/2015ef000347.

Byrnes, M.R., Griffee, S.F., Osler, M.S., 2010, September. Channel Dredging and Geomorphic Response at and Adjacent to Mobile Pass, Alabama. U.S. Army Corps of Engineers. http://hdl.handle.net/11681/7722.

Chettiyam Thodi, M.F., Gopinath, G., Surendran, U.P., Prem, P., Al-Ansari, N., Mattar, M. A., 2023. Using RS and GIS techniques to assess and monitor coastal changes of coastal islands in the marine environment of a humid tropical region. Water 15 (21), 3819. https://doi.org/10.3390/w15213819.

Dauphin Island Sea Lab & Alabama Department of Conservation and Natural Resources (DCNR), 2018. Alabama State Expenditure Plan (SEP). https://restorethegulf.gov/spill-impact-component/alabama.

Durán, O., Moore, L.J., 2013. Vegetation controls on the maximum size of coastal dunes. Proc. Natl. Acad. Sci. 110 (43), 17217–17222. https://doi.org/10.1073/pnas.1307580110.

Feagin, R.A., Figlus, J., Zinnert, J.C., Sigren, J., Martínez, M.L., Silva, R., Smith, W.K., Cox, D., Young, D.R., Carter, G., 2015. Going with the flow or against the grain? The promise of vegetation for protecting beaches, dunes, and barrier islands from erosion. Front. Ecol. Environ. 13 (4), 203–210. https://doi.org/10.1890/140218.

Fernández-Montblanc, T., Duo, E., Ciavola, P., 2020. Dune reconstruction and revegetation as a potential measure to decrease coastal erosion and flooding under extreme storm conditions. Ocean Coast. Manag. 188, 105075. https://doi.org/10.1016/j.ocecoaman.2019.105075.

Gopinath, G., Chettiyam Thodi, M.F., Surendran, U.P., Prem, P., Parambil, J.N., Alataway, A., Al-Othman, A.A., Dewidar, A.Z., Mattar, M.A., 2023. Long-term shoreline and islands change detection with digital shoreline analysis using RS data and GIS. Water 15 (2), 244. https://doi.org/10.3390/w15020244.

Gornish, E.S., Miller, T.E., 2022. Whole plant traits of coastal dune vegetation and implications for interactions with dune dynamics. Ecol. Appl. 32 (6), e2643. https://doi.org/10.1002/eap.2643.

Guy, K.K., 2015a. Barrier Island shorelines extracted from Landsat imagery. In: Open-File Report. https://doi.org/10.3133/ofr20151179.

Guy, K.K., 2015b. Shorelines Extracted from Landsat Imagery. U.S. Geological Survey data release, Petit Bois Island, Mississippi. https://doi.org/10.5066/F72N509Q.

Guy, K.K., 2015c. Shorelines Extracted from Landsat Imagery: Horn Island, Mississippi [Data Set]. U.S. Geological Survey. https://doi.org/10.5066/F7XW4GVG.

Han, S., 2021. The use of transects for resilient design: core theories and contemporary projects. Landsc. Ecol. 36, 1567–1582. https://doi.org/10.1007/s10980-020-01172-9.

Han, S., Hogue, W., 2024. Assessing human influence and vegetative dune dynamics on barrier islands via satellite raster classification. Environ. Manag. 1-14. https://doi.org/10.1007/s00267-024-02038-5.

Hanley, M., Hoggart, S., Simmonds, D., Bichot, A., Colangelo, M., Bozzeda, F., Heurtefeux, H., Ondiviela, B., Ostrowski, R., Recio, M., Trude, R., Zawadzka-Kahlau, E., Thompson, R., 2014. Shifting sands? Coastal protection by sand banks, beaches, and dunes. Coast. Eng. 87, 136–146. https://doi.org/10.1016/j.coastaleng.2013.10.020.

Henderson, R.E., Nelson, P.R., Long, J.W., Smith, C., 2017. Vector Shorelines and Associated Shoreline Change Rates Derived from Lidar and Aerial Imagery for Dauphin Island, Alabama: 1940–2015. U.S. Geological Survey data release. https://doi.org/10.5066/F7T43RB5.

Himmelstoss, E.A., Henderson, R.E., Kratzmann, M.G., Farris, A.S., 2018. Digital shoreline analysis system (DSAS) version 5.0 user guide. U.S. Geol. Surv. Open-File Report 2018–1179, 110. https://doi.org/10.3133/ofr20181179.

Himmelstoss, E., Henderson, R., Kratzmann, M., Farris, A., 2021. Digital Shoreline Analysis System (DSAS) version 5.1 user guide. In: U.S. Geological Survey Open-File Report 2018–1179, p. 104, 10.3133/ofr20211091.

Irish, J.L., Frey, A.E., Rosati, J.D., Olivera, F., Dunkin, L.M., Kaihatu, J.M., Ferreira, C.M., Edge, B.L., 2010. Potential implications of global warming and barrier island degradation on future hurricane inundation, property damages, and population impacted. Ocean Coast. Manag. 53 (10), 645–657. https://doi.org/10.1016/j.ocecoaman.2010.08.001.

Masselink, G., Ruju, A., Conley, D., Turner, I., Ruessink, G., Matias, A., Wolters, G., 2016. Large-scale barrier dynamics experiment II (BARDEX II): experimental design, instrumentation, test program, and data set. Coast. Eng. 113, 3–18. https://doi.org/10.1016/j.coastaleng.2015.07.009.

Miller, D., Thetford, M., Verlinde, C., Campbell, G., Smith, A., University of Florida, Institute of Food and Agricultural Sciences, Florida Sea Grant College, 2018. Dune

Restoration and Enhancement for the Florida Panhandle. Amsterdam University Press.
Morton, R.A., 2008. Historical changes in the Mississippi-Alabama barrier-island chain and the roles of extreme storms, sea level, and human activities. J. Coast. Res. 24 (6), 1587–1600. https://doi.org/10.2112/07-0953.1.
Passeri, D.L., Hagen, S.C., Medeiros, S.C., Bilskie, M.V., 2015. Impacts of historic morphology and sea level rise on tidal hydrodynamics in a microtidal estuary (Grand Bay, Mississippi). Cont. Shelf Res. 111, 150–158. https://doi.org/10.1016/j.csr.2015.08.001.
Sancho, F., Abreu, T., D'Alessandro, F., Tomasicchio, G.R., Silva, P.A., 2011. Surf hydrodynamics in front of collapsing coastal dunes. J. Coast. Res. 144–148. https://www.jstor.org/stable/26482150.
Schmid, M., Kutser, T., Kutnar, L., 2024. Containing alien plants in coastal dunes: evidence from a soil manipulation experiment. J. Environ. Manag. 350, 121780. https://doi.org/10.1016/j.jenvman.2024.121780.
Seabloom, E.W., et al., 2024. Impact of invasive *Carex kobomugi* on the native dune community structure and sediment dynamics. Ecosphere 15 (1), e4065. https://doi.org/10.1002/ecs2.4065.
Smith, C.G., Long, J.W., Henderson, R.E., Nelson, P.R., 2018, November. Assessing the Impact of Open-ocean and Back-barrier Shoreline Change on Dauphin Island, Alabama, at Multiple Time Scales over the last 75 years. U.S. Geological Survey. https://doi.org/10.3133/ofr20181170.
Stallins, J.A., 2005. Stability domains in barrier island dune systems. Ecol. Complex. 2 (4), 410–430. https://doi.org/10.1016/j.ecocom.2005.04.011.
U.S. Geological Survey, 2007. Historical Shoreline Changes and Associated Coastal Land Loss along the U.S. Gulf of Mexico: 1800s to 2004 (open-file report 2007–1161). https://pubs.usgs.gov/of/2007/1161/.
U.S. Geological Survey, 2020. Dauphin Island Conceptual Ecological Model. Gulf of Mexico Ecological Services Division. https://gom.usgs.gov/DauphinIsland/data/AppL_CEMDauphinIsland_2020April20_Final.pdf.
U.S. Geological Survey, 2023. Digital Shoreline Analysis System (DSAS) version 5.1 user guide: A Tool for Calculating Shoreline Change Statistics (Open-File Report 2023–1011, by Himmelstoss, E. A., Henderson, R. E., Kratzmann, M. G., Farris, A. S., Zichichi, J. L., & Thieler, E. R.). U.S. Department of the Interior. https://doi.org/10.3133/ofr20231011.